Biochemical and Biophysical Research Communications 441 (2013) 425–430

Contents lists available at ScienceDirect

Biochemical and Biophysical Research Communications

journal homepage: www.elsevier.com/locate/ybbrc

Combined small RNA and degradome sequencing reveals microRNA regulation during immature maize embryo dedifferentiation

Yaou Shen [a,1], Zhou Jiang [a,1], Sifen Lu [b], Haijian Lin [a], Shibin Gao [a], Huanwei Peng [c], Guangsheng Yuan [a], Li Liu [a], Zhiming Zhang [a], Maojun Zhao [d], Tingzhao Rong [a], Guangtang Pan [a,*]

[a] Maize Research Institute, Sichuan Agricultural University, Chengdu 611130, China
[b] BGI, Shenzhen 518083, China
[c] Institute of Animal Nutrition, Sichuan Agricultural University, Ya'an 625014, China
[d] College of Life and Science, Sichuan Agricultural University, Ya'an 625014, China

ARTICLE INFO

Article history:
Received 29 September 2013
Available online 30 October 2013

Keywords:
Maize
Immature embryo
Dedifferentiation
Small RNA sequencing
Degradome sequencing
miRNA regulation

ABSTRACT

Genetic transformation of maize is highly dependent on the development of embryonic calli from the dedifferentiated immature embryo. To better understand the regulatory mechanism of immature embryo dedifferentiation, we generated four small RNA and degradome libraries from samples representing the major stages of dedifferentiation. More than 186 million raw reads of small RNA and degradome sequence data were generated. We detected 102 known miRNAs belonging to 23 miRNA families. In total, we identified 51, 70 and 63 differentially expressed miRNAs (DEMs) in the stage I, II, III samples, respectively, compared to the control. However, only 6 miRNAs were continually up-regulated by more than fivefold throughout the process of dedifferentiation. A total of 87 genes were identified as the targets of 21 DEM families. This group of targets was enriched in members of four significant pathways including plant hormone signal transduction, antigen processing and presentation, ECM-receptor interaction, and alpha-linolenic acid metabolism. The hormone signal transduction pathway appeared to be particularly significant, involving 21 of the targets. While the targets of the most significant DEMs have been proved to play essential roles in cell dedifferentiation. Our results provide important information regarding the regulatory networks that control immature embryo dedifferentiation in maize.

1. Introduction

As a major agricultural crop, maize provides protein and energy for human and livestock nutrition and therefore is one of the prime targets for genetic manipulation. Genetic transformation of maize requires the formation of embryonic calli derived from the dedifferentiated immature embryos. However, there are clear differences in dedifferentiation frequency among various genotypes. Only a few maize lines display high frequency of induction of embryonic calli [1]. We previously investigated the transcriptional changes that occur during immature maize embryo dedifferentiation at genome-wide level and identified important genes and pathways involved in embryonic callus formation [2]. However, it is still unclear how the genes and pathways are regulated during the dedifferentiation process.

miRNAs are a large group of small endogenous RNAs found in animals, plants and some viruses [3]. Increasing evidence indicates that plant miRNAs play important regulatory roles in many biological and metabolic processes, including plant development, hormone signaling, and responses to environmental stress [4–6]. However, miRNAs do not directly control plant growth and development. In contrast, miRNAs affect plant phenotypes by repressing functional gene expression. Bartel (2004) predicted the targets of 16 miRNAs in *Arabidopsis*, and 70% of these targets have since been implicated in the control of plant development or cell differentiation [7]. So far, the majority of the known plant miRNAs have been isolated from differentiated tissues or organs such as leaves, roots, tassels, ears and pollens [8,9]. Consequently, very few miRNAs

Abbreviations: ARF, auxin response factor; CK, the control; DEM, differentially expressed miRNA; Dicer, double-stranded-specific RNase; GA, gibberellin; HLH, helix-loop-helix; MFE, minimum free energy; miRNA, microRNA; NAM, no apical meristem; QTL, quantitative trait locus; RPM, reads per million clean reads.

* Corresponding author. Address: 46#, Xinkang Road, Ya'an 625014, Sichuan Province, China. Fax: +86 835 2882714.

E-mail addresses: shenyaou@gmail.com (Y. Shen), jiangzhou@126.com (Z. Jiang), lusifen@genomics.org.cn (S. Lu), linhj521@gmail.com (H. Lin), shibingao@163.com (S. Gao), phwly02@aliyun.com (H. Peng), yuangs_032@163.com (G. Yuan), liuli198411@163.com (L. Liu), zhangzm1979@aliyun.com (Z. Zhang), zmjun01@yahoo.com.cn (M. Zhao), rongtz@sicau.edu.cn (T. Rong), pangt@sicau.edu.cn (G. Pan).

[1] These authors contribute equally to this work.

0006-291X/$ - see front matter © 2013 Elsevier Inc. All rights reserved.
http://dx.doi.org/10.1016/j.bbrc.2013.10.113

associated with an undifferentiated state have been identified. It is unknown how miRNA expression changes during the process of tissue or organ dedifferentiation in plants.

To identify miRNAs and their targets involved in immature embryo dedifferentiation, we constructed small RNA and degradome libraries of four major developmental stages from differentiated immature embryo to undifferentiated callus. A total of 23 conserved miRNA families were detected. We identified 87 genes targeted by the DEMs, determined the most significantly regulated pathway enriched with the target genes, and experimentally verified the function of the hormone pathway in dedifferentiation. While the targets of the most significant DEMs have been proved to play essential roles in cell dedifferentiation. Taken together, these findings provide important information regarding regulatory networks involved in immature embryo dedifferentiation in maize.

2. Materials and methods

2.1. Samples and RNA isolation

The process of immature embryo dedifferentiation in 18-599R was divided into three major stages based on morphological features: embryo intumescence (stage I, 1–5 d), initial callus formation (stage II, 6–10 d), and embryonic callus generation (stage III, 11–15 d) in our previous work [2]. In the present study, line 18-599R was grown under the condition as reported in the previous research. Total RNA was isolated from a pool of 30 embryos or calli from each sample from 0 to 15 d, using Trizol Reagent (Invitrogen) according to the manufacturer's instructions. RNA from non-cultured immature embryos (0 d) was used as a control (CK). RNA taken from 1 to 5 d old samples was mixed in equal proportions, as well as 6–10 d old samples and 11–15 d samples. The three RNA samples and the control were then submitted to the construction of small RNA and degradome libraries.

2.2. Small RNA library construction and identification of conserved maize miRNAs

Small RNA libraries were constructed using the Small RNA Sample Prep Kit (Illumina) as described by Tang et al. (2012) [10]. Briefly, 100 μg of total RNA was run on a 15% Acrylamide/8 M Urea gel, and small RNAs (18–30 nt) were extracted and ligated to a 5′ RNA adapter and a 3′ RNA adapter. cDNA libraries were then constructed by reverse transcription using SuperScript™ III (Invitrogen) and enriched by 15 cycles of PCR. The final PCR products were then purified using the PureLink™ PCR Purification Kit (Invitrogen) and sequenced by Solexa technology. Small RNA reads were processed using the FASTX-Toolkit to remove adapter sequences and low quality reads. Then, we compared the remaining sequences that were between 18 and 30 nt against the miRNA database (miRBase 20 released) in maize (http://www.mirbase.org). Only perfect matches were designated as conserved miRNAs.

2.3. Identification of differentially expressed miRNAs

The number of absolute sequence reads of miRNAs in each library was converted to normalized abundance of miRNAs by converting the data into "reads per million clean reads (RPM)". The calculation of the *p*-value for comparison of the miRNA expression between the stage samples and the control sample was performed based on previously established methods [11]. In detail, the $\log_2$ ratio formula was: $\log_2$ ratio = $\log_2$ (miRNA reads in stage sample/miRNA reads in control). The following formula was used to calculate *p*-value:

$$p(x|y) = \left(\frac{N_2}{N_1}\right)^y \frac{(x+y)!}{x!y!\left(1+\frac{N_2}{N_1}\right)^{(x+y+1)}}$$

N_1 and N_2 denote the total number of reads in two compared libraries, respectively, while x and y represents the number of reads of an miRNA in the two libraries. *p*-Value indicates the significance of prospect differences of miRNA abundance. A combination of $p < 0.01$ and the absolute value of $\log_2$ ratio $\geqslant 1$ were used as the threshold to determine the significance of gene expression difference.

2.4. Degradome library construction and identification of miRNA targets

Degradome libraries were constructed as described by [12]. In brief, polyadenylated RNA was purified from 200 μg of total RNA using the Oligotex Kit (Qiagen). T4 RNA ligase was used to ligate a 5′ RNA adapter with a MmeI recognition site to the 5′ terminus of the poly(A) RNA. The resulting products were repurified using Oligotex Kit, reversely transcribed with by five PCR cycles, digested with *Mme* I, and ligated to a 3′ double DNA adapter. Finally, the ligated products were amplified with 20 PCR cycles and gel-purified for deep sequencing. The raw sequences were using the Fastx-Toolkit, then normalized to reads per million (RPM). The remaining sequences were unique reads that perfectly matched maize cDNA sequences listed in WMD3 database (http://wmd3.weigelworld.org). CleaveLand was used to identify the targets cleaved by the maize miRNAs identified in our study [13].

2.5. Real-time PCR

Verification of the maize miRNA expression patterns was carried out by RNA-tailing and primer-extension reverse transcription RT-PCR [3]. Briefly, reverse transcription was performed using 1 μg of poly(A)-tailed small RNA and 1 μg of RT primer [5′-GCTGTCAACGATACGCTACGTAACGGCATGACAGTG-d(T)(A, G, or C)-3′] with 200 U of SuperScript III (Invitrogen). Next, quantitative real-time PCR was performed using Bio-Rad CFX96 with 5s rRNA (gi: 114151623) as the endogenous control. The primers were designed using Beacon Designer 7 software and are listed in Supplemental Table S1. The standard Bio-Rad CFX96 amplification conditions were used: an initial denaturation at 98 °C for 2 min, then 40 cycles of 98 °C for 2 s and 59 °C for 10 s, followed by a thermal denaturation step to generate the melting curves to verify the amplification specificity. Three biologically independent replicates were performed for all reactions, including non-template controls. Statistical analysis was performed using the $2^{-\Delta\Delta CT}$ method.

2.6. Determining the functions of the targets of differentially expressed miRNAs

The functions of the targets of miRNAs that were up- or down-regulated significantly between the dedifferentiation stages and the CK samples were determined using NCBI COG (http://www.ncbi.nlh.nih.gov/COG), the Gene Ontology Database (http://www.geneontology.org/) and KEGG pathway (http://genome.jp/keg/) [14].

3. Results and discussion

3.1. Small RNAs involved in immature embryo dedifferentiation

The inbred maize line 18-599R is an excellent model for immature embryo dedifferentiation and the induction of embryonic callus [2]. We constructed 4 small RNA libraries from the embryos

and the calli at the three typical stages of dedifferentiation. After removing the low quality sequences, adapter sequences and sequences smaller than 18 nt, 17,155,464 (99.63%), 15,829,092 (99.78%), 16,750,312 (99.74%), and 15,279,493 (99.70%) clean reads remained from the control, stage I, stage II, and stage III samples. RNAs between 21 and 22 nt were the second or third most abundant sequences in the libraries (Fig. 1), in which 1,807,025 (10.53%), 2,035,514 (12.85%), 2,427,490 (14.48%), and 2,788,805 (18.23%) sequences was 21-nt in the four samples. These RNAs are the typical length of mature plant miRNAs. The results are consistent with deep sequencing results from other plants [8,15]. We further obtained 4,890,526, 6,102,061, 7,003,679, and 5,551,340 unique reads from the clean reads. Among them, 2,850,709 (58.29%), 3,501,509 (57.38%), 4,281,020 (61.13%), and 3,104,611 (55.935) unique reads were specifically expressed in the control, stage I, stage II, stage III libraries, respectively, and only 727,034 (less than 14.87%) unique reads were expressed in all of the four samples (Fig. 2). These results indicated that the expression of small RNA changes significantly during dedifferentiation of the immature maize embryo.

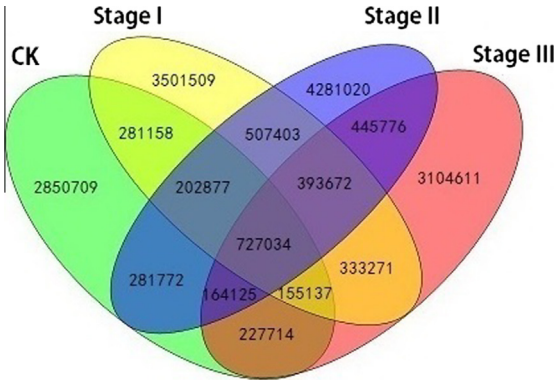

Fig. 2. Venn-diagram for the comparison of the four small RNA populations. The numbers of the unique reads were compared among CK and the stage samples. The four-way Venn-diagram indicates the numbers of the unique reads in CK (green oval), stage I (yellow oval), stage II (blue oval) and stage III (red oval). The numbers inside the intersections of the ovals denote the numbers of the unique reads identified in two, three, or four small RNA libraries. (For interpretation of the references to colour in this figure legend, the reader is referred to the web version of this article.)

3.2. miRNA families identified in maize

A total of 172 miRNAs belonging to 29 families in maize have been deposited in the current database miRBase 20 released (June 24, 2013). We detected 102 of these known miRNAs belonging to 23 families, but did not detect 70 of them that included all of the members of the miR395, miR482, miR1432, miR2118 and miR2275 families. The number of absolute sequence reads of miRNAs was transformed to normalized abundance of miRNAs by converting the data into "reads per million clean reads (RPM)" (Supplemental Table S2). Based on the normalized abundance, miR156, miR166, miR168 and miR528 were the most highly expressed miRNA families, with more than 10,000 RPM each in at least one sample. Whereas, miR162 was low abundance miRNA, with less than 1 RPM in each of the samples (Supplemental Fig. S1).

3.3. Differentially expressed miRNAs over the course of immature embryo dedifferentiation

We analyzed changes in miRNA expression levels during the process of dedifferentiation. The miRNAs whose expression levels changed significantly ($p < 0.01$, with absolute values of $\log_2$ (ratio) $\geqslant 1$) between the control sample and the samples from the three different stages are shown in Supplemental Table S3. Overall, the expression level of 51, 70, and 63 miRNAs significantly up- or down-regulated compared to the control during stage I, stage II, stage III, respectively. A total of 30, 38, 53 miRNAs were separately up-regulated, whereas 21, 32, 10 miRNAs were down-regulated in the stage samples compared to the control. Among them, miR164e, miR169c,r, miR529 and miR528a,b were the most significantly differentially expressed miRNAs, and were gradually up-regulated by more than fivefold d throughout the process of dedifferentiation.

3.4. Validation of immature maize embryo miRNAs

To validate the miRNA expression detected by deep sequencing technology, 11 miRNA sequences (miR156a,b,c,d,e,f,g,h,l, miR160-a,b,c,d,e,g, miR167a,b,c,d, miR168a,b, miR319a,b,c,d, miR393a,c, miR396a,b, miR397a,b, miR528a,b, miR827) were randomly selected for quantitative real-time PCR analysis. The expression level in the stage I, stage II and stage III samples were compared to CK. As shown in Fig. 3, there was a strong correlation (Pearson's correlation > 0.90) between the deep sequencing data and quantitative real-time PCR analysis, indicating the reliability of both of the methods.

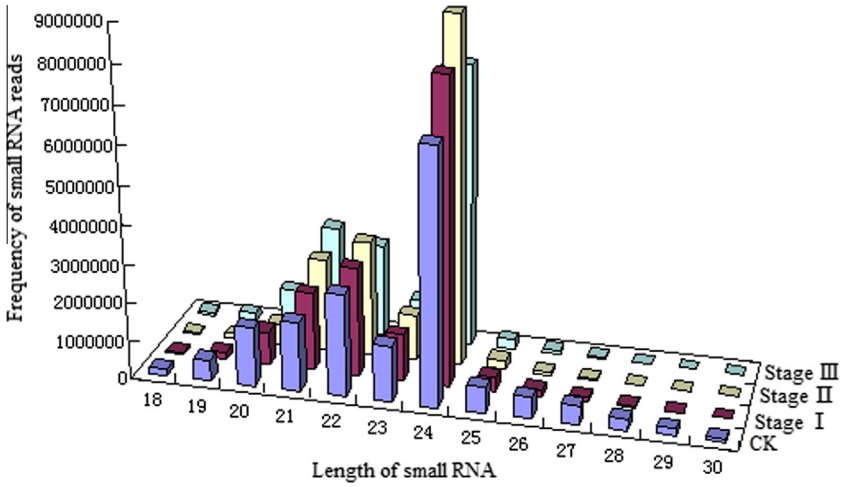

Fig. 1. The size distribution of small RNA. Numbers on the abscissa axis and *y*-axis represent the length of small RNA sequence and frequency of small RNA reads, respectively.

3.5. Immature embryo dedifferentiation degradomes

Degradome sequencing technology was applied to identify the targets of the DEMs in our study. In total, 22,376,272 (99.3%), 30,334,985 (99.1%), 35,800,265 (99.2%), and 32,067,467 (99.2%) clean reads were obtained, including 8,681,692, 5,872,016, 12,163,352, and 11,165,771 unique reads respectively. Using BLASTn to search against the Rfam database, we further exclude known noncoding RNAs (rRNA, tRNA, snRNA, and snoRNA), which represented 0.25%, 0.33%, 0.30%, 0.26% of the unique signature data sets. The rest of the reads were then mapped to the maize genome. Altogether, 5,887,373 (67.8%), 3,759,318 (64.0%), 7,840,829 (64.5%), and 7,370,944 (66.0%) unique reads had perfect matches in the maize genome (Table 1). These results correlated well with a previous study in soybeans [10,12]. Reads from the degradome library containing polyadenylated fragments were considered to be noise. However, less than 0.1% of unique reads ended with poly(A), which is lower than the percentage of polyadenylated reads present in the wheat degradome library. These results demonstrate the high quality of maize degradome libraries developed in this study.

3.6. DEM targets identified by degradome sequencing

We identified miRNA targets based on the following criteria suggested by Allen et al., Schwab et al. and Shuai et al. [9,16,17]: (1) the cleaved region of mRNA should be complementary to the miRNA sequence; (2) all alignments must have scores of no more than four, where one mismatch between the miRNA and the target sequence counts was counted as one, and G/U bases count as 0.5 score; (3) the cleavage site should generally fall between the 10th and 11th nt in the miRNA sequence, and there can be no mismatches at the cleavage site; (4) no more than two adjacent mismatches are allowed in the miRNA/target duplex; (5) no more than 2.5 mismatches should occur at positions 1–12 nt (from the 5′ end of miRNA) of the miRNA/target duplex; (6) the minimum free energy (MFE) of the miRNA/target duplex should be equal to or greater than 74% of the MFE of the miRNA bound to its perfect complement.

The target transcripts were sorted into four categories according to the abundance of miRNA-complemented signatures compared to other signatures mapped to the same mRNA, as described by Song et al. (2011) [12]. Briefly, an miRNA-cleavaged signature which was the only cleavage signature of the transcript was classified as Category 0. For Category I, the expected cleavage signature was equal to the maximum among all cleavage signatures of the transcript. In Category II, the abundance of miRNA-mediated cleavage signatures was less than the maximum but higher than the median. The signatures with an abundance less than or equal to the median were grouped into Category III. All of the identified miRNA target transcripts were classified according to these criteria. A total of 164 transcripts representing 87 genes were identified as the targets of 17 known DEM families (Supplemental Table S4). Notably, dozens of transcription factors as GAMYB, TCP, SBP and ARF were identified as the targets of miR319, miR156, miR160 and miR167, respectively, which have been experimentally validated by the previous studies [18–20]. Approximate 70.0% of the target transcripts belonged to Category 0 or I in at least one sample, and the proportion is even higher than those observed in previous researches [9,12]. Taken together, these findings provide important evidence on the high reliability of target identification in the present research.

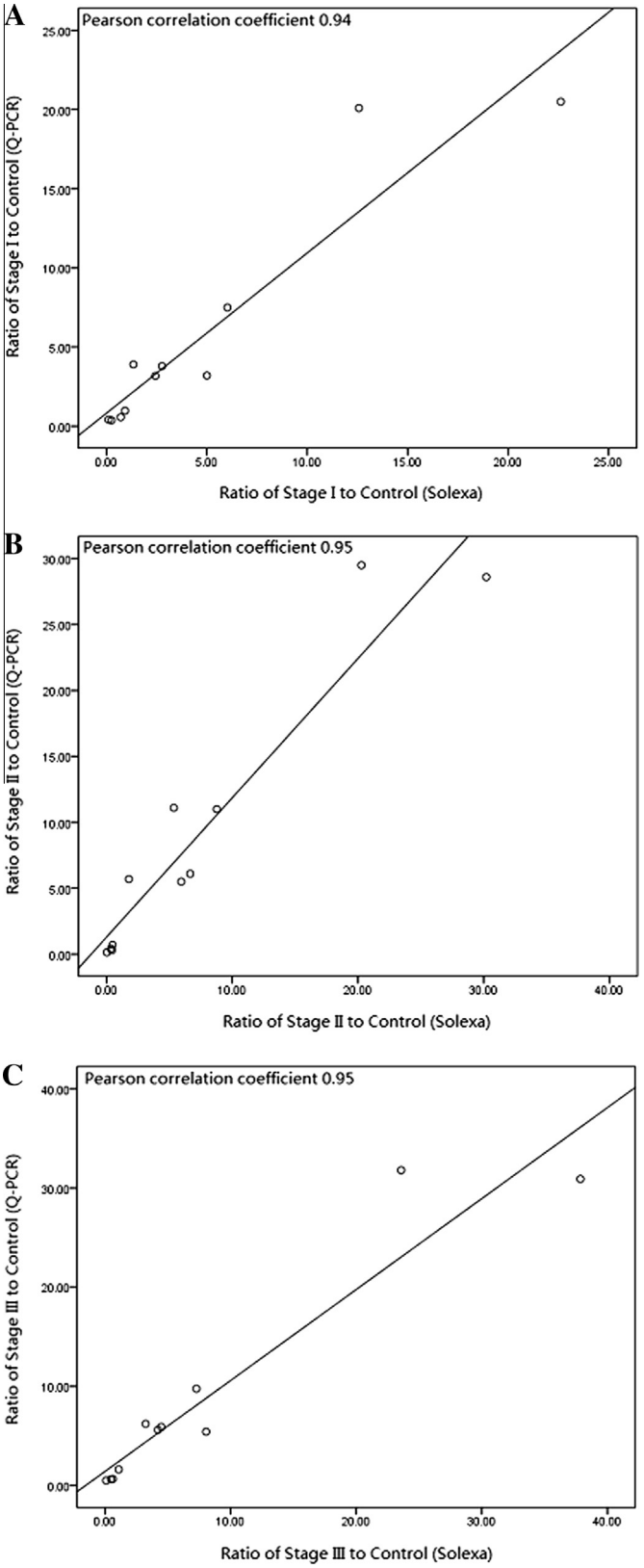

Fig. 3. Correlations of expression ratios of miRNAs between Q-PCR and deep sequencing in the three stages. A, B and C denote stage I, stage II and stage III, respectively, and the numbers on *x*-axis and *y*-axis represent the detected ratios of expression levels of the stage sample to CK by the method of deep sequencing and Q-PCR, respectively.

Table 1
Summary of the degradome library reads.

Sample	Raw reads	Clean reads	Unique reads	Genome mapped reads	cDNA mapped reads	Exon mapped reads	Intron mapped reads
Control	22,527,288	22,376,272	8,681,692	5,887,373	5,485,192	3,412,497	611,651
Stage I	30,603,839	30,334,985	5,872,016	3,759,318	3,518,660	2,228,365	403,414
Stage II	36,095,716	35,800,265	12,163,352	7,840,829	7,039,337	4,546,600	950,635
Stage III	32,319,190	32,067,467	11,165,771	7,370,944	6,771,178	4,527,062	848,678

3.7. Pathways regulated by DEMs during immature embryo dedifferentiation

To shed more light on the functional role of miRNAs in immature embryo dedifferentiation, we identified biological pathways enriched with DEM targets. We found that the targets were involved in members of four significant ($p < 0.01$) pathways including plant hormone signal transduction, antigen processing and presentation, ECM-receptor interaction, and alpha-linolenic acid metabolism (Supplemental Table S5). The plant hormone signal transduction pathway [21,22] was the most highly relevant pathway, with 21 genes involved. In detail, there were 13 (TIR1: GRMZM2G137451, GRMZM2G135978; ARF: GRMZM2G078274, GRMZM2G035405, GRMZM2G390641, GRMZM2G028980, AC207656.3_FG002, GRMZM2G081406, GRMZM2G159399, GRMZM2G089640, GRMZM2G475882, GRMZM2G153233, GRMZM2G081158), 8 (DELLA: GRMZM2G418899, GRMZM2G037792, GRMZM2G079470, GRMZM5G825321, GRMZM2G110579, GRMZM2G098800; TF gene: GRMZM2G028054, GRMZM2G139688) genes that participates in the secondary pathways of auxin signal transduction and gibberellin (GA) signal transduction, respectively (Fig. 4). Auxin is considered to be the main hormone involved in plant dedifferentiation process [23], and 2, 4-D, an auxin analogue, is widely considered to be the most important exogenous hormone for use in immature embryo dedifferentiation [24]. In a recent study, auxin pathway mediated by miRNAs was revealed to play an important role during cotton somatic embryogenesis [25]. GAs can regulate growth, including stem elongation, germination in plants [26], and bioactive GA accumulate as maize embryogenesis proceeded [27]. Whereas, inhibitions of embryogenesis and germination are required for the process of immature embryo dedifferentiation. All of the above findings are in accordance with our findings well, which validates the significant regulation of miRNAs on plant dedifferentiation by promoting auxin signal pathway and repressing the GA pathway.

3.8. Function of targets of the most significantly differentially expressed miRNAs

Although 21 of 29 miRNA families were all differentially expressed during immature embryo dedifferentiation (Supplemental Table S3), only six miRNAs (miR164e, miR169c/r, miR528a/b and miR529) (approximate 3.5%) were continually up-regulated by more than fivefold throughout the process, suggesting that these miRNAs might be primarily responsible for immature embryo dedifferentiation. A total of 16 genes were identified as the targets of them (Supplemental Table S4), separately, including 2 *NAM* (No Apical Meristem) gene, 2 SBP transcription factors, 1 HLH transcription regulator, 1 Ribosomal_S12, 1 F-box protein GID2, 1 HVA22-like protein a, and 8 unknown transcription factors. *NAM* genes are expressed at the boundaries between organ primordial and meristems, and play a role in determining the positions of meristems and primordia [28]. In addition, NAM proteins are required for pattern formation in *Petunia* embryos, and *Petunia* embryos carrying the *nam* mutation fail to develop a shoot apical meristem [29]. In this study, we found that miR164 which targets the *NAM* gene was the most significantly differentially expressed DEM, and was continually up-regulated by more than sevenfold throughout the process of dedifferentiation. It is suggested that miR164 is one of the key miRNAs related to immature embryo dedifferentiation in maize. HLH transcription factors are a family of proteins containing helix-loop-helix structural motifs [30]. The function of HLH transcription factors on plant cell dedifferentiation is still unclear, but numbers of researches have proved that HLH transcription factors acted as inhibitors of differentiation in human and animal cells. The kinds of proteins play important roles in

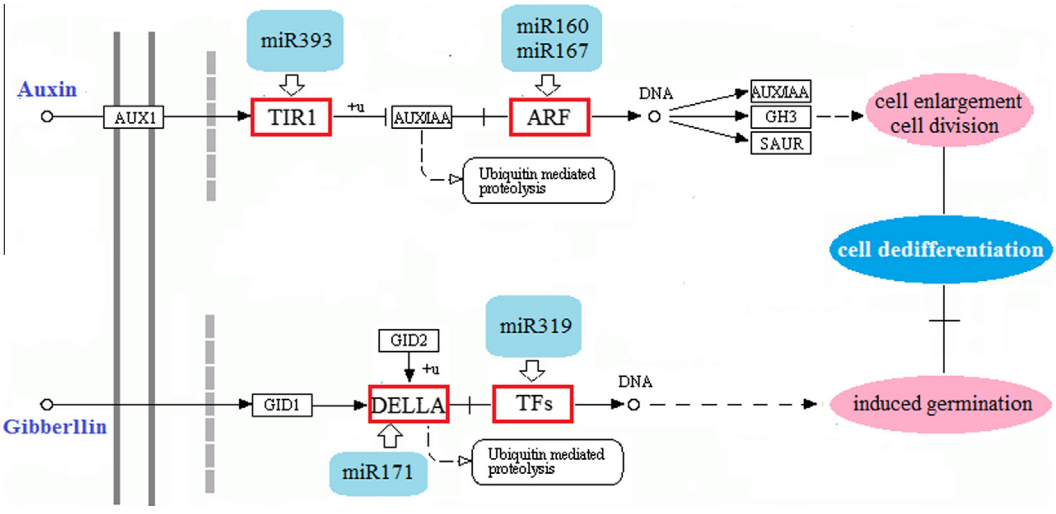

Fig. 4. Pathway of the plant hormone signal transduction regulated by the DEMs. These genes in red panes denote maize genes that participate in the auxin and GA signal transduction, and they were targets of the DEMs identified in the study. MiRNAs in blue panes indicate the miRNAs targeting these genes. (For interpretation of the references to colour in this figure legend, the reader is referred to the web version of this article.)

control of cell division [31], inhibition of cell differentiation [32], and drive of cell dedifferentiation [33]. Here we report a HLH transcription factor in maize regulated by miR528, which may be a new breakthrough point in the research of plant dedifferentiation. We would therefore propose the miRNAs participate in immature embryo dedifferentiation of maize by regulating some key genes controlling the process.

Acknowledgments

This study was supported by the National Natural Science Foundation of China (31271739), the Project of Transgenic New Variety Cultivation (2013ZX08003-003) and Major Project of Education Department in Sichuan (11ZA087).

Appendix A. Supplementary data

Supplementary data associated with this article can be found, in the online version, at http://dx.doi.org/10.1016/j.bbrc.2013.10.113.

References

[1] Y. Wu, L. Yuan, X. Guo, D.R. Holding, J. Messing, Mutation in the seed storage protein kafirin creates a high-value food trait in sorghum, Nat. Commun. 4 (2013) 2217.
[2] Y. Shen, Z. Jiang, X. Yao, Z. Zhang, H. Lin, M. Zhao, H. Liu, H. Peng, S. Li, G. Pan, Genome expression profile analysis of the immature maize embryo during dedifferentiation, PLoS One 7 (2012) e32237.
[3] Y. Shen, Z. Zhang, H. Lin, H. Liu, J. Chen, H. Peng, M. Cao, T. Rong, G. Pan, Cytoplasmic male sterility-regulated novel microRNAs from maize, Funct. Integr. Genomics 11 (2011) 179–191.
[4] B.J. Reinhart, E.G. Weinstein, M.W. Rhoades, B. Bartel, D.P. Bartel, MicroRNAs in plants, Genes Dev. 16 (2002) 1616–1626.
[5] J. Zhang, Y. Xu, Q. Huan, K. Chong, Deep sequencing of *Brachypodium* small RNAs at the global genome level identifies microRNAs involved in cold stress response, BMC Genomics 10 (2009) 449.
[6] Y. Ding, Y. Tao, C. Zhu, Emerging roles of microRNAs in the mediation of drought stress response in plant, J. Exp. Bot. 65 (2013) 3077–3086.
[7] D.P. Bartel, MicroRNAs: genomics, biogenesis, mechanism, and function, Cell 116 (2004) 281–297.
[8] C.Z. Zhao, H. Xia, T.P. Frazier, Y.Y. Yao, Y.P. Bi, A.Q. Li, M.J. Li, C.S. Li, B.H. Zhang, X.J. Wang, Deep sequencing identifies novel and conserved microRNAs in peanuts (*Arachis hypogaea* L.), BMC Plant Biol. 10 (2010) 3.
[9] P. Shuai, D. Liang, Z. Zhang, W. Yin, X. Xia, Identification of drought-responsive and novel *Populus trichocarpa* microRNAs by high-throughput sequencing and their targets using degradome analysis, BMC Genomics 14 (2013) 233.
[10] Z. Tang, L. Zhang, C. Xu, S. Yuan, F. Zhang, Y. Zheng, C. Zhao, Uncovering small RNA-mediated responses to cold stress in a wheat thermosensitive genic male-sterile line by deep sequencing, Plant Physiol. 159 (2012) 721–738.
[11] S. Audic, J.M. Claverie, The significant of digital gene expression profiles, Genome Res. 7 (1997) 986–995.
[12] Q.X. Song, Y.F. Liu, X.Y. Hu, W.K. Zhang, B. Ma, S.Y. Chen, J.S. Zhang, Identification of miRNAs and their target genes in developing soybean seeds by deep sequencing, BMC Plant Biol. 11 (2011) 5.
[13] C. Addo-Quaye, W. Miller, M.J. Axtell, CleavaLand: a pipeline for using degradome data to find cleaved small RNA targets, Bioinformatics 25 (2009) 130–131.
[14] Y. Shen, Y. Zhang, J. Chen, H. Lin, M. Zhao, H. Peng, L. Liu, G. Yuang, S. Zhang, Z. Zhang, G. Pan, Genome expression profile analysis reveals important transcripts in maize roots responding to the stress of heavy metal Pb, Physiol. Plant. 147 (2013) 270–282.
[15] Z. Xie, E. Allen, N. Fahlgren, A. Calamar, S.A. Givan, J.C. Carrington, Expression of *Arabidopsis* MIRNA genes, Plant Physiol. 138 (2010) 2145–2154.
[16] E. Allen, Z. Xie, A.M. Gustafson, J.C. Carrington, MicroRNA-directed phasing during trans-acting siRNA biogenesis in plants, Cell 121 (2005) 207–221.
[17] R. Schwab, J.F. Palatnik, M. Riester, C. Shommer, M. Schmid, D. Weigel, Specific effects of microRNA on the plant transcriptome, Dev. Cell 8 (2005) 517–527.
[18] F. Thiebaut, C.A. Rojas, K.L. Almeida, C. Grativol, G.C. Domiciano, C.R. Lamb, A. Engler Jde, A.S. Hemerly, P.C. Ferreira, Regulation of miR319 during cold stress in sugarcane, Plant Cell Environ. 35 (2012) 502–512.
[19] C. Schommer, J.F. Palatnik, P. Aggarwal, A. Chételat, P. Cubas, E.E. Farmer, U. Nath, D. Weigel, Control of jasmonate biosynthesis and senescence by miR319 targets, PLoS Biol. 6 (2008) e230.
[20] S. Xing, M. Salinas, S. Höhmann, R. Berndtgen, P. Huijser, MiR156-targeted and nontargeted SBP-box transcription factors act in concert to secure male fertility in *Arabidopsis*, Plant Cell 22 (2010) 3935–3950.
[21] N. Dharmasiri, S. Dharmasiri, M. Estelle, The F-box protein TIR1 is an auxin receptor, Nature 435 (2005) 441–445.
[22] J. Kim, K. Harter, A. Theologis, Protein–protein interactions among the Aux/IAA proteins, Proc. Natl. Acad. Sci. USA 94 (1997) 11786–11791.
[23] X. Yang, X. Zhang, D. Yuan, F. Jin, Y. Zhang, J. Xu, Transcript profiling reveals complex auxin signalling pathway and transcription regulation involved in dedifferentiation and redifferentiation during somatic embryogenesis in cotton, BMC Plant Biol. 12 (2012) 110.
[24] T.P. Pasternak, E. Prinsen, F. Ayaydin, P. Miskolczi, G. Potters, H. Asard, H.A. Van Onckelen, D. Dudits, A. Fehér, The role of auxin, pH, and stress in the activation of embryogenic cell division in leaf protoplast-derived cells of alfalfa, Plant Physiol. 129 (2002) 1807–1819.
[25] X. Yang, L. Wang, D. Yuan, K. Lindsey, X. Zhang, Small RNA and degradome sequencing reveal complex miRNA regulation during cotton somatic embryogenesis, J. Exp. Bot. 64 (2013) 1521–1536.
[26] M. Ogawa, A. Hanada, Y. Yamauchi, A. Kuwahara, Y. Kamiya, S. Yamaguchi, Gibberellin biosynthesis and response during *Arabidopsis* seed germination, Plant Cell 15 (2003) 1591–1604.
[27] C.N. White, C.J. Rivin, Gibberellins and seed development in maize. II. Gibberellin synthesis inhibition enhances abscisic acid signaling in cultured embryos, Plant Physiol. 122 (2000) 1089–1098.
[28] X. Cheng, J. Peng, J. Ma, Y. Tang, R. Chen, K.S. Mysore, J. Wen, No Apical Meristem (MtNAM) regulates floral organ identity and lateral organ separation in *Medicago truncatula*, New Phytol. 195 (2012) 71–84.
[29] E. Souer, A. Van Houwelingen, D. Kloos, J. Mol, R. Koes, The no apical meristem gene of *Petunia* is required for pattern formation in embryos and flowers and is expressed at meristem and primordia boundaries, Cell 85 (1996) 159–170.
[30] M.E. Massari, C. Murre, Helix-loop-helix proteins: regulators of transcription in eukaryotic organisms, Mol. Cell. Biol. 20 (2000) 429–440.
[31] B.V. Fausett, J.D. Gumerson, D. Goldman, The proneural basic helix-loop-helix gene Ascl1a is required for retina regeneration, J. Neurosci. 28 (2008) 1109–1117.
[32] T. Ogata, J.M. Wozney, R. Benezra, M. Noda, Bone morphogenetic protein 2 transiently enhances expression of a gene, Id (inhibition of differentiation), encoding a helix-loop-helix molecule in osteoblast-like cells, Proc. Natl. Acad. Sci. USA 90 (1993) 9219–9222.
[33] Y. Li, J. Yang, J. Luo, S. Dedhar, Y. Liu, Tubular epithelial cell dedifferentiation is driven by the helix-loop-helix transcriptional inhibitor Id1, J. Am. Soc. Nephrol. 18 (2007) 449–460.